Radial Flows Over a Horizontal Plate

A.J. ROBERTS and D.V. STRUNIN
Department of Mathematics and Computing
University of Southern Queensland
Toowoomba, Queensland 4350
AUSTRALIA
aroberts@usq.edu.au; strunin@usq.edu.au

Abstract: A circular jump forms in the radial flow thickness when a downwards stream hits a horizontal plate. Centre manifold theory is used to rigorously derive, from the Navier-Stokes equations, a dynamic model for slow horizontal variations of flow thickness and velocity. An advantage of this approach is the capacity to study non-stationary regimes and examine stability of the flow. Numerical solutions of the model reproduce experimentally observed recirculation under the jump and quantitatively agree with experiments of laminar flows.

Key-Words: Radial fluid flow, hydraulic jump, centre manifold.

1 Introduction

A fluid jet impinging downwards onto a horizontal surface generates a flow with hydraulic jump, that is, a sudden elevation of a free surface of fluid [1]–[3]. For certain parameters of the flow the jump is stationary and radially symmetric. The phenomenon has been studied theoretically in many works but there is still lack of systematic approach to the dynamics.

One of the most simple models of the hydraulic jump is an inviscid flow exhibiting Rayleigh's shock [4]. Linear one-dimensional shocks are considered in early work by Rayleigh [5], where, in particular, river bores were analyzed as moving shocks. The basic assumptions of this model are continuity of mass and momentum fluxes across the shock, but discontinuity of kinetic energy flux. It was shown that in order to meet a natural requirement that the kinetic energy be lost in the shock, the free surface behind the shock must be higher then before. There have been attempts to use this approach together with potential theory to model circular hydraulic jumps [6]–[7]. However, this gave incorrect predictions for the radius of the jump. It was found that the radius should essentially depend on the radius of the falling jet and, hence, on the radius of a nozzle where the jet discharges from. Experiments have not confirmed such a dependence. A more elaborate model by Watson [6] suggested that part of the flow is effectively viscous and part effectively inviscid. For the viscid segment, a similarity velocity profile was prescribed. This theory also treated the hydraulic jump as the shock. The viscous part was shown to play substantial role in the dynamics. The model was simplified by Tani [8] who supposed the flow was totally viscid. The boundary layer equations were averaged over the depth of the flow under assumption of similarity velocity profile. Bohr et al. [7] developed this approach further, and good predictions for the radius of the jump were obtained.

There are two main shortcomings of these models — they describe only stationary states and they are heuristic: as mentioned above, vertical velocity profiles are often approximated by similarity distributions. For example, Bohr et al. [7] assumed a parabolic structure: $u(r,z) = \bar{u}(C_1\zeta - C_2\zeta^2)$, $\zeta = z/\eta(r)$, where $\bar{u}$ is the depth-average velocity, r is the radius, z is the vertical coordinate, η is the flow thickness, and C_1, C_2 are some constant coefficients.

In this paper we use an approach that rests on the solid basis of centre manifold theory. Its detailed description can be found, for instance, in [9]. Here we briefly outline the main idea of this theory. Consider a dynamical system

$$\dot{x} = Ax + f(x,y,a)\,, \quad \dot{y} = By + g(x,y,a)\,, \quad (1)$$

where the overdot denotes d/dt, a is a set of parameters, x and y are generally multidimensional variables, and f and g are nonlinear functions. It is assumed that the eigenvalues of the $m \times m$ matrix A all have zero real part, and the eigenvalues of the $n \times n$ matrix B all have strictly negative real part. Near the origin $(x, y, a) = (0, 0, 0)$ the *linear* dynamics dominate and the modes y are driven exponentially quickly to 0 due to the equations $\dot{y} = By$. These modes are thus ignored when considering the linear long-term evolution, and the dynamics are approximately described in terms of the *neutral* modes, x, which obey the equations $\dot{x} = Ax$. Then centre manifold theory asserts that this linear picture is only modified by the nonlinear terms f and g: the modes $y(t)$ go exponentially quickly to a manifold $y = h(x, a)$, called the centre manifold; and thereafter the long-term evolution of the system is described by the low-dimensional system $\dot{x} = Ax + f(x, h, a)$. Centre manifold theory has been successfully applied to a number of problems such as dispersion of contaminants in channels [10], [11], dynamics of thin films on inclined planes [12] and others.

2 Centre manifold model

Li and Roberts [13] used the centre manifold technique to describe thin fluid flows on curved substrates. In particular, their model is applicable to flows on plane surfaces, which interest us here. A similar approach was earlier used by Roberts [12]. Let us describe the main points of the approach. The fluid dynamics are governed by the continuity equation and Navier-Stokes equations:

$$\nabla \cdot \mathbf{u} = 0\,, \tag{2}$$

$$\frac{\partial \mathbf{u}}{\partial t} + \mathbf{u} \cdot \nabla \mathbf{u} = -\frac{1}{\rho}\nabla p + \frac{\mu}{\rho}\nabla^2 \mathbf{u} + \mathbf{g}\,, \tag{3}$$

where traditional notations are used. Attached to (2)–(3) are boundary conditions expressing no slip on the bottom plate, the free surface kinematic relation, a jump in normal stress on the free surface caused by surface tension, and zero tangential stress on the surface. The dimensional equations (2)–(3) are non-dimensionalized using characteristic thickness of the film, H, as the reference length; $\mu H/\sigma$, where σ is the coefficient of surface tension, as the reference time; σ/μ as the reference velocity; and σ/H as the reference pressure. The non-dimensional form of (2)–(3) is

$$\nabla \cdot \mathbf{u} = 0\,, \tag{4}$$

$$R\left[\frac{\partial \mathbf{u}}{\partial t} + \mathbf{u} \cdot \nabla \mathbf{u}\right] = -\nabla p + \nabla^2 \mathbf{u} + B\mathbf{g}\,, \tag{5}$$

where $\mathbf{g}$ is a unit gravitational vector, $R = \sigma\rho H/\mu^2$ is the Reynolds number, and $B = \rho g H^2/\sigma$ is the Bond number.

To set the equations to a form treatable by the centre manifold approach Roberts [12] performed the following tricks. First, the horizontal gradients, $\partial/\partial x$ and $\partial/\partial y$, are supposed small: $\partial/\partial x \sim \varepsilon$, $\partial/\partial y \sim \varepsilon$ (non-dimensional), where ε is a small parameter. Second, the gravitational force is regarded as a perturbing "nonlinear" term by introducing small parameter β such that $B = \beta^2$. Third, the tangential stress on the free surface is modified using an artificial parameter γ so that at $\gamma = 0$ the lateral shear mode of slowest decay actually becomes a neutral mode, but at $\gamma = 1$ the tangential stress boundary condition is recovered. The idea is to seek a solution as power series in γ, ε and β and substitute $\gamma = 1$ into final expressions in order to model the original physical problem. Convergence of the series at $\gamma = 1$ is confirmed by calculations [13]. According to the centre manifold technique the horizontal velocity components u and v, vertical velocity w and pressure p are represented as functions of "amplitudes" of the neutral modes: these are η and, as measures of the velocity, the horizontal depth-average velocity components $\bar{u}$ and $\bar{v}$. Centre manifold theory guarantees that the solution is representable in the form

$$\begin{aligned} &\mathbf{u}(t) = \mathbf{U}(\eta, \bar{u}, \bar{v})\,, \\ &\text{such that} \quad \frac{\partial}{\partial t}\begin{bmatrix}\eta \\ \bar{u} \\ \bar{v}\end{bmatrix} = \mathbf{G}(\eta, \bar{u}, \bar{v})\,. \end{aligned} \tag{6}$$

In (6) the dependence on the parameters ε, γ and β is implicit. By adjoining the trivial equations

$$\partial\varepsilon/\partial t = 0\,, \quad \partial\gamma/\partial t = 0\,, \quad \partial\beta/\partial t = 0$$

a new dynamical system is obtained for $\mathbf{u}$, η, p, ε, γ and β. Once the terms of the original dynamical system involving parameters ε and β are treated as small perturbations, the theory leads to a physically adequate solution for slow horizontal variations (small ε), and a relatively weak gravitational force (small β).

Analyzing (4), (5), (6) using computer algebra yields the model [13]

$$\frac{\partial \eta}{\partial t} \approx -\frac{\partial(\eta\bar{u})}{\partial x} - \frac{\partial(\eta\bar{v})}{\partial y}\,, \tag{7}$$

$$\begin{aligned} R\frac{\partial \bar{u}}{\partial t} \approx & -\frac{\pi^2}{4}\frac{\bar{u}}{\eta^2} + \frac{\pi^2}{12}Bg\eta_x \\ & -R\left[1.5041\bar{u}\frac{\partial \bar{u}}{\partial x} + 1.3464\bar{v}\frac{\partial \bar{u}}{\partial y} + 0.1577\bar{u}\frac{\partial \bar{v}}{\partial y}\right. \\ & \left. +0.1483\frac{\bar{u}}{\eta}(\bar{u}\eta_x + \bar{v}\eta_y)\right] \\ & + \left[4.0930\frac{\partial^2 \bar{u}}{\partial x^2} + \frac{\partial^2 \bar{u}}{\partial y^2} + 3.0930\frac{\partial^2 \bar{v}}{\partial x \partial y}\right. \\ & +4.8333\frac{\eta_x}{\eta}\frac{\partial \bar{u}}{\partial x} + \frac{\eta_y}{\eta}\frac{\partial \bar{u}}{\partial y} + 1.9167\frac{\eta_x}{\eta}\frac{\partial \bar{v}}{\partial y} + 1.9167\frac{h_y}{\eta}\frac{\partial \bar{v}}{\partial x} \\ & + \left(-0.5033\frac{\eta_y^2}{\eta^2} - \frac{\eta_{yy}}{2\eta} + 0.1061\frac{\eta_x^2}{\eta^2} - 0.5834\frac{\eta_{xx}}{\eta}\right)\bar{u} \\ & \left. + \left(0.6094\frac{\eta_y\eta_x}{\eta^2} - 0.0833\frac{\eta_{xy}}{\eta}\right)\bar{v}\right]\,, \end{aligned} \tag{8}$$

$$\begin{aligned} R\frac{\partial \bar{v}}{\partial t} \approx & -\frac{\pi^2}{4}\frac{\bar{v}}{\eta^2} + \frac{\pi^2}{12}Bg\eta_y \\ & -R\left[1.3464\bar{u}\frac{\partial \bar{v}}{\partial x} + 1.5041\bar{v}\frac{\partial \bar{v}}{\partial y} + 0.1577\bar{v}\frac{\partial \bar{u}}{\partial x}\right. \\ & \left. +0.1483\frac{\bar{v}}{\eta}(\bar{u}\eta_x + \bar{v}\eta_y)\right] \\ & + \left[\frac{\partial^2 \bar{v}}{\partial x^2} + 4.0930\frac{\partial^2 \bar{v}}{\partial y^2} + 3.0930\frac{\partial^2 \bar{u}}{\partial x \partial y}\right. \\ & +4.8333\frac{\eta_y}{\eta}\frac{\partial \bar{v}}{\partial y} + \frac{\eta_x}{\eta}\frac{\partial \bar{v}}{\partial x} + 1.9167\frac{\eta_x}{\eta}\frac{\partial \bar{u}}{\partial y} + 1.9167\frac{h_y}{\eta}\frac{\partial \bar{u}}{\partial x} \\ & + \left(-0.5033\frac{\eta_x^2}{\eta^2} - \frac{\eta_{xx}}{2\eta} + 0.1061\frac{\eta_y^2}{\eta^2} - 0.5834\frac{\eta_{yy}}{\eta}\right)\bar{v} \\ & \left. + \left(0.6094\frac{\eta_y\eta_x}{\eta^2} - 0.0833\frac{\eta_{xy}}{\eta}\right)\bar{u}\right]\,, \end{aligned} \tag{9}$$

In this paper we confine our attention to radially-symmetric flows. To transform (8) and (9) to radial geometry, polar coordinates $x = r\cos\varphi$, $y = r\sin\varphi$ should be used under assumption that η, $\bar{u}$ and $\bar{v}$ do not depend on φ. The equations for the radial flow are presented further below.

Meanwhile, the characteristic dimensional scales adopted in [13] are inconvenient for the particular problem. The scales are essentially based on the surface tension coefficient, σ, which has a negligible role in the radial dynamics, at least for the flows reported in [1]. We choose different characteristic scales which are typical for the problem in question: radius r_*, thickness η_*, velocity u_*, pressure $p_* = \rho g r_*$ and time $t_* = r_*/u_*$. These values are estimated from the governing equations as follows. Assuming that in the Navier-Stokes equations the non-stationary term, inertia terms, pressure term and viscous term are all of the same order of magnitude one gets

$$\frac{u_*}{t_*} = \frac{u_*^2}{r_*} = \frac{u_* w_*}{\eta_*} = \frac{\rho g \eta_*}{\rho r_*} = \frac{\nu u_*}{\eta_*^2}\,, \tag{10}$$

where $\nu = \mu/\rho$. The mass flux relation gives

$$u_* r_* \eta_* = Q\,, \tag{11}$$

(Q equals the total mass flux divided by 2π), and the continuity relation gives

$$\frac{u_*}{r_*} = \frac{w_*}{\eta_*}\,. \tag{12}$$

Solving (10)–(12) results in

$$r_* = \left(\frac{Q^5}{\nu^3 g}\right)^{1/8}\,, \quad u_* = \left(Q\nu g^3\right)^{1/8}\,. \tag{13}$$

Using scales (13) we deduce new non-dimensional form of the equations (2)–(3):

$$\nabla \cdot \mathbf{u} = 0\,, \tag{14}$$

$$\frac{\partial \mathbf{u}}{\partial t} + \mathbf{u}\cdot\nabla\mathbf{u} = -\frac{1}{Fr}\nabla p + \frac{1}{Re}\nabla^2\mathbf{u} + \frac{\mathbf{g}}{Fr}\,, \tag{15}$$

where the Froude number Fr and the new Reynolds number Re are:

$$Fr = \frac{u_*^2}{g r_*}\,, \quad Re = \frac{r_* u_*}{\nu}\,. \tag{16}$$

Substituting (13) into (16) we reveal that the Froude and Reynolds numbers are represented in terms of a single parameter which is the non-dimensional total mass flux q:

$$Re = 1/q^2\,, \quad Fr = q\,, \quad q = \frac{\nu^{5/8}}{Q^{3/8} g^{1/8}}\,. \tag{17}$$

Let us show that the expression for q indeed represents the non-dimensional mass flux. Label temporarily the dimensional quantities by tildes to distinguish them from dimensionless quantities.

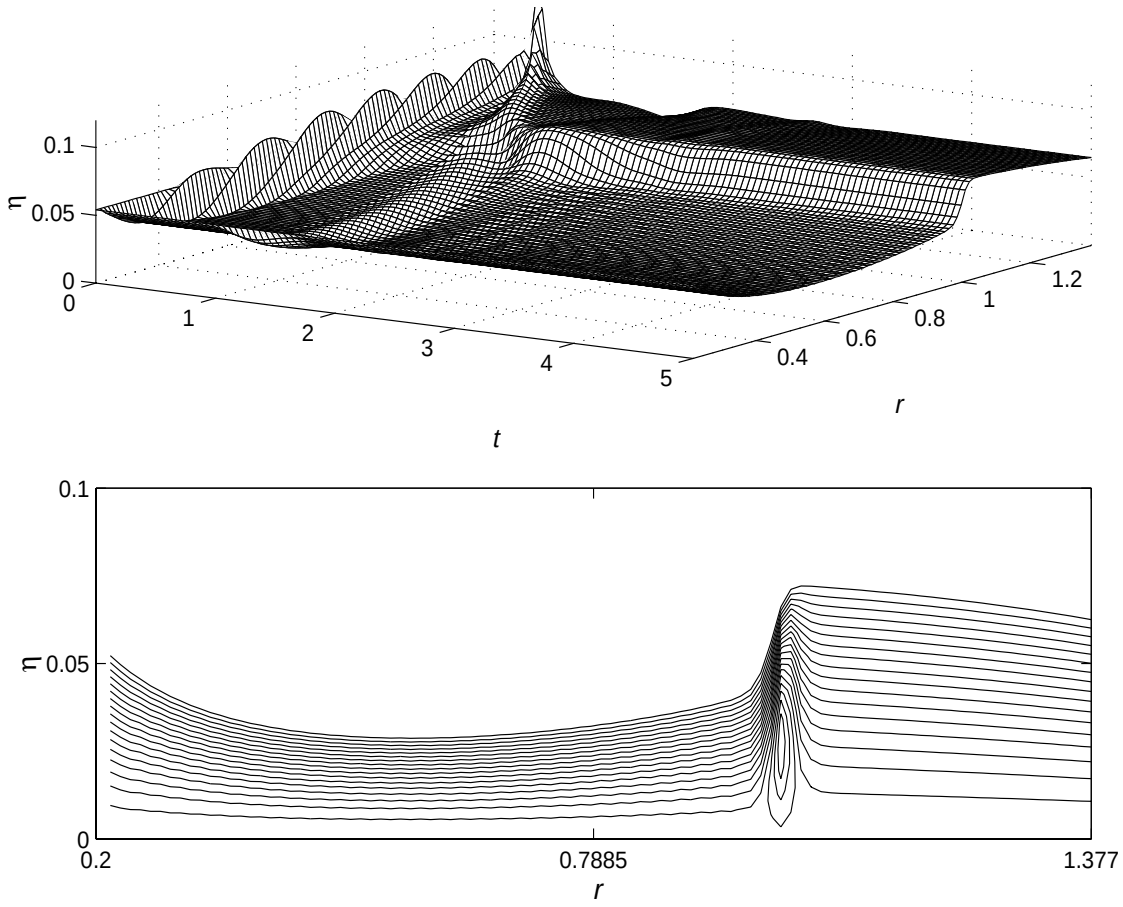

Figure 1: $\bar{U}_2 = 0.55$. The flow evolves to stationary state. Streamlines of the eventual flow pattern show recirculation under the jump.

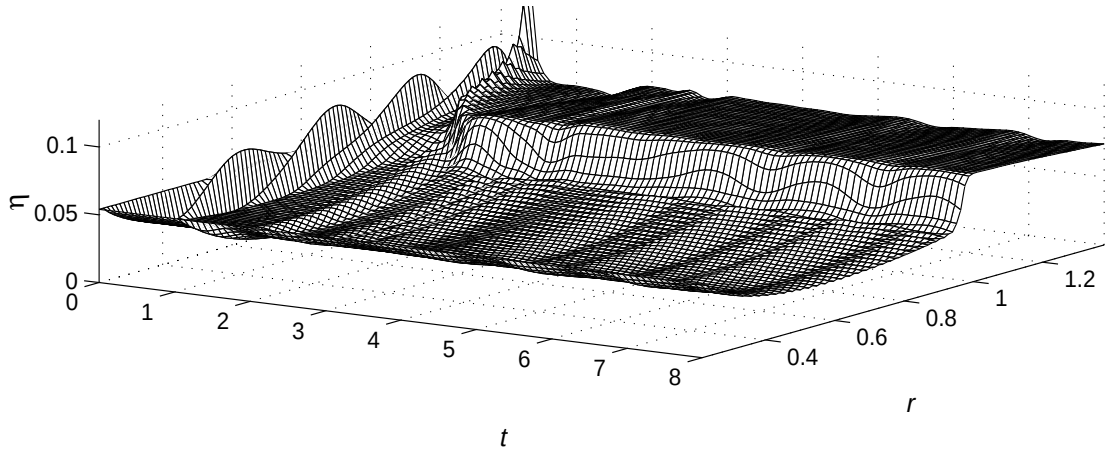

Figure 2: $\bar{U}_2 = 0.48$. The flow evolves to a settled oscillating regime.

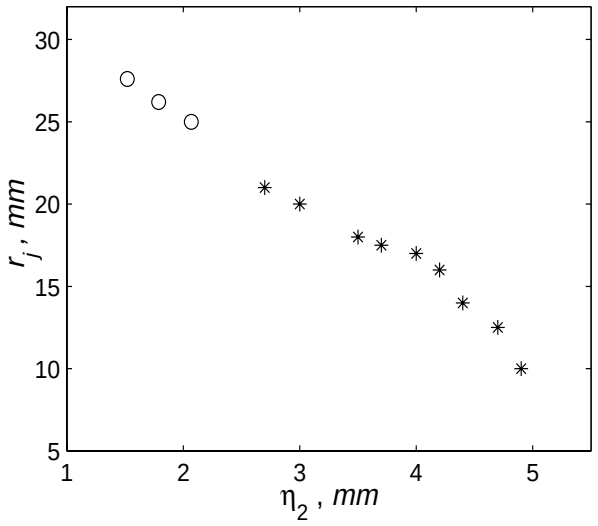

Figure 3: The position of the stationary jump versus the external thickness. Stars are plotted using Fig. 3 of [1], circles correspond to our model.

By definition $q = ru\eta$, therefore, $q = (\tilde{r}/r_*)(\tilde{u}/u_*)(\tilde{\eta}/r_*) = (\tilde{r}\tilde{u}\tilde{\eta})/(r_*^2 u_*) = Q/(r_*^2 u_*)$. Substituting here (13) we readily obtain the above formula for q. Computer algebra yields (the same result follows from (7)–(9)):

$$\frac{\partial \eta}{\partial t} \approx -\frac{1}{r}\partial_r(r\bar{U}\eta)\,, \tag{18}$$

$$\begin{aligned}\frac{\partial \bar{U}}{\partial t} \approx & -2.4674\,q^2\frac{\bar{U}}{\eta^2} \\ & +1.4166\,q^2\frac{\eta_r}{r\eta}\bar{U} - 0.8225\,q^{-1}\eta_r \\ & -1.5041\bar{U}\bar{U}_r - 0.1577\frac{1}{r}\bar{U}^2 - 0.1483\frac{\eta_r}{\eta}\bar{U}^2 \\ & +4.0930\,q^2\,\partial_r\left\{\frac{1}{r}\partial_r(r\bar{U})\right\} + 4.8333\,q^2\frac{\eta_r}{\eta}\bar{U}_r \\ & +\left(0.1066\,q^2\frac{\eta_r^2}{\eta^2} - 0.5834\,q^2\frac{\eta_{rr}}{\eta}\right)\bar{U}\,,\end{aligned} \tag{19}$$

where $\bar{U}$ is the average radial velocity ($\bar{U}^2 = \bar{u}^2 + \bar{v}^2$). See that the continuity equation is of the first order in r and the momentum equation is of the second order in r. Hence, we need three boundary conditions. We choose these to specify velocity and film thickness on the left end of spatial domain, that is at some relatively small fixed radius r_1, and velocity on the right end, that is at some fixed $r_2 > r_1$.

3 Numerical results

We solved equations (18)–(19) using the DAE2 solver developed by Roberts [14]. To compare numerical results with the experiments we used dimensional parameters from [1] which were the same in all the computations: $r_1 = 6$ mm, $\eta_1 = 1.5$ mm, $r_2 = 38$ mm, and $Q = 27/(2\pi)$ ml/s. Once the total flux, coordinate and thickness on the left end are stipulated, then the velocity on this end is obtained from the continuity condition as $\bar{U}_1 = Q/(\eta_1 r_1)$. Thus, the boundary conditions on the left end were fixed, while the boundary condition specifying the velocity on the right end, $\bar{U}_2$, was free to be varied on our choice from one experiment to another. Various magnitudes of $\bar{U}_2$ lead to various thicknesses on the right end, η_2. In some sources this thickness is called external height. In the laboratory experiments [1] η_2 was controlled by the height of a circular rim surrounding the falling jet. Because the hydraulic jump is formed far away from the rim, the rim does not act as *immediate* cause of the jump; it only controls the right end boundary condition. Note that the jump is formed even when there is no rim. The initial condition was chosen to represent uniform thickness throughout the flow and velocity decreasing like $1/r$. The latter choice provided a constant mass flux at the initial moment, which helped reduce oscillations in early stages of the dynamics. We adopted

$$\eta(r,0) \equiv \eta_1\,, \quad \bar{U}(r,0) = q/(r\eta_1)\,.$$

For $\bar{U}_2 > 0.5$ we observed that stationary flow is eventually formed after some transitional evolution. An example of the flow dynamics and eventual streamline pattern is shown in Fig. 1. In the jump area a vortex (recirculation area) is situated, where fluid particles move along closed orbits. This feature qualitatively agrees with the laboratory observations. For $\bar{U}_2 < 0.5$ unsteady behaviour of the flow is obtained (Fig. 2).

Depending on the controlling boundary value of the velocity from the range $\bar{U}_2 > 0.5$ the flow settles upon a certain thickness after the jump, η_2, and certain jump coordinate r_j. The comparison of the numerical and experimental results for the stationary flows are presented in Fig. 3. See that the points representing numerical solutions form one line with the points representing experiments.

The unsteady regimes at relatively large values of η_2 ($\bar{U}_2 < 0.5$) can be explained by too abrupt change in the flow thickness and velocity in the jump area. The larger η_2 the larger the spatial derivatives entering the governing equations. Recall that the accuracy of these equations is assured by the centre manifold theory provided the spatial variations are slow enough. This condition is violated for extremely steep jumps. To extend the area of applicability of the centre manifold model, it is necessary to take into account higher-order terms in ε. Nevertheless, for relatively small external heights the model works well, and stability of the solution is demonstrated by Fig. 1.

4 Conclusion

A non-stationary radial model of thin fluid flow is developed to study the circular hydraulic jump formed by a stream of fluid hitting a horizontal plate. Accuracy of the model, for smooth flows, is assured by the centre manifold theory. Stationary flow patterns are obtained for relatively small external heights. For the stationary regimes, the dependence of jump location against the external height is determined, showing good agreement with available experimental data. Stability of the regimes is demonstrated. The model well reproduces a recirculation zone under the hydraulic jump.

Acknowledgement. We thank the ARC for support of this research.

References

[1] T. Bohr, C. Ellegaard, A.E. Hansen and Haaning, Hydraulic jumps, flow separation and wave breaking: an experimental study, *Physica B*, Vol.228, 1996, pp. 1–10.

[2] T. Bohr, C. Ellegaard, A.E. Hansen, K. Hansen, A. Haaning, V. Putkaradze and S. Watanabe, Separation and pattern formation in hydraulic jumps, *Physica A*, Vol.249, 1998, pp. 111–117.

[3] C. Ellegaard, A.E. Hansen, K. Hansen, A. Haaning, A. Marcussen, T. Bohr, J. Lundbeck Hansen and S. Watanabe, Creating corners in kitchen sinks, *Nature*, Vol.392, 1998, p. 767.

[4] V.T. Chow, *Open-channel hydraulics*, McGraw-Hill, 1959.

[5] O.M. Rayleigh, On the theory of long waves and bores, *Proc. Roy. Soc.*, Vol.A90, 1914, pp. 324–328.

[6] E.J. Watson, The radial spread of a liquid jet over a horizontal plane, *J. Fluid Mech.*, Vol.20, 1964, pp. 481–499.

[7] T. Bohr, P. Dimon and V. Putkaradze, Shallow-water approach to the circular hydraulic jump, *J. Fluid Mech.*, Vol.254, 1993, pp. 635–648.

[8] I. Tani, Water jump in the boundary layer, *J. Phys. Soc. Japan*, Vol.4, 1949, pp. 212–215.

[9] J. Carr, *Applications of centre manifold theory*, Springer-Verlag, 1981.

[10] G.N. Mercer and A.J. Roberts, A centre manifold description of contaminant dispersion in channels with varying flow properties, *SIAM J. Appl. Math.*, Vol.50, 1990, pp. 1547–1565.

[11] A.J. Roberts and D.V. Strunin, Rigorous zonal model of contaminant dispersion in shear flows, In: *Recent Advances in Applied and Theoretical Mathematics*, Ed. N.E. Mastorakis (WorldSES Press, Athens, Greece, 2000) pp. 64–70.

[12] A.J. Roberts, Low-dimensional models of thin film fluid dynamics, *Phys. Lett. A*, Vol.212, 1996, pp. 63–71.

[13] Z. Li and A.J. Roberts, The accurate and comprehensive model of thin fluid flows with inertia on curved substrates, *University of Southern Queensland Working Paper Series*, SC-MC-9909, 1999.

[14] A.J. Roberts, *http://www.sci.usq.edu.au/staff/robertsa/*.